SIMULATION OF TRAILING EDGE SCATTERING BY USING ACOUSTIC/VISCOUS SPLITTING METHODS WITH OVERSET GRID TECHNIQUES

Yonghwan Park[*], Jonghoon Bin[*], Cheolung Cheong[#] and Soogab Lee[†]
School of Mechanical and Aerospace Engineering
Seoul National University
Seoul 151-742, Korea

ABSTRACT

Receptivity of steady shear flows is the main issues for analysis overall acoustic scattering for airfoil trailing edge and near-nozzle lip. This paper focuses on the development of accurate and robust numerical methods to accompany high-order computational aeroacoustics algorithms towards the simulation of trailing edge scattering problem in Category 4 and on the analysis of the generation mechanism of the instability wave by the interaction of trailing edge, shear layer and initial disturbance. The numerical methods is based on Grid-Optimized Dispersion-Relations-Preserving (GODRP) schemes developed with grid-optimization algorithm to make finite difference equations possess the same dispersion relations as the corresponding partial differential equations on general geometries. Acoustic/viscous splitting techniques, based on flow noise solvers using acoustic governing equations such as simplified linearized Euler equations and full linearized Euler equations, are utilized to solve the receptivity by the interactions of trailing edge, shear layer and initial disturbance. The numerical analysis consists of two steps. First, steady mean flow is determined by solution of the compressible Navier-Stokes equation using Roe's scheme for spatial discretization and local time stepping for time discretization. Then, unsteady trailing edge scattering phenomena are simulated with the CAA solvers. Through the comparison of acoustic simulations, it will be shown that mean flow gradient terms play a crucial role in triggering the instability wave

1. INTRODUCTION

At subsonic flow, one of the primary sources of trailing edge noise corresponds to receptivity, excitation of shear layer. The various mechanisms contributing to such receptivity on trailing edge include the interaction between vortices, shear layer, and unsteady disturbances. Especially, in the receptivity process, shear layer instability waves are generated (ref. 1). These waves excite shear layer and produce sound. The noise generated by these phenomena has become an important issue for the design of engine, nozzle and airfoil trailing edge.

In the present decade, considerable progress in computational aeroacoustics (CAA) has been achieved. The unsteady governing equations are discretized and solved for time-dependent flow variables, which includes the mean flow and the flow or acoustic disturbances. High-order schemes are required for discretization to reduce dissipation and dispersion errors. Recently, Grid-Optimized Dispersion-Relation-Preserving (GODRP) scheme (ref. 2) have been developed with the grid-optimization algorithm to make the finite difference equations possess the same dispersion relations as the corresponding partial differential equations and, at the same time, optimized dissipation characteristics at the given grids that are the non-uniform Cartesian or curvilinear grids. In this work, the GODRP schemes are utilized to solve this complex geometry problem with curvilinear grids on a guarantee of local and, thus resultant global dispersion-relation-preserving properties. In addition, high-order schemes support the formation of spurious modes at the boundaries of the computational domain. Careful attention for unsteady boundary treatment is needed to produce the physically correct disturbance field. Therefore, accurate nonreflecting boundary conditions are necessary for computational aeroacoustics. The sponge zone technique by Baily & Bogey

[*] Ph. D. Candidate, qwer1104@snu.ac.kr
[*] Ph. D. Candidate, mrbin@snu.ac.kr
[#] BK21 Post Doctor, accu99@snu.ac.kr
[†] Professor, solee@plaza.snu.ac.kr, Bldg. 301-1303, Seoul National University, Seoul 151-742, Korea

(ref. 3) is used with the nonreflecting boundary condition of Tam & Dong(ref. 4) as the inflow/outflow boundary conditions.

Acoustic/viscous splitting technique is utilized for the analysis of the receptivity phenomena. These methods are based on the concept of variable decomposition in the governing equations into a source component and an acoustic one, which leads to two separate sets of equations governing viscous flow field and acoustic disturbance field, respectively. This approach is based on the assumption that the wave propagation is essentially inviscid in nature and sound perturbations are so small that their contribution to the convection velocity of the flow is negligible in most cases. The most important advantage of the decomposition method is that algorithms are used that best suited to each solver: traditional CFD algorithms for the viscous flow and CAA algorithms for the acoustic perturbations.

It is very difficult to construct a single body-fitted mesh for thin plate which gives the proper resolution to both the near source region and far acoustic field. This difficulty is overcome by the use of a multi-scale overset grid technique, where body-fitted meshes are applied only near the plate and Cartesian background mesh is applied elsewhere.

Problem statement will be briefly demonstrated in Section 2. The numerical methods together with the governing equations and numerical boundary treatment will be discussed in Section 3, which is followed by numerical results and discussion will be provided in Section 4.

2. PROBLEM STATEMENT

This benchmark problem consists of a two-dimensional compressible mixing layer flow formed by a splitter plate with blunt trailing edge. First, a steady laminar mixing layer solution is determined by 2D compressible laminar Navier-Stokes equation.

$$\frac{\partial U}{\partial t}+\frac{\partial F}{\partial x}+\frac{\partial G}{\partial y}=\frac{\partial V_x}{\partial x}+\frac{\partial V_y}{\partial y} \tag{1}$$

where $\mathbf{U}=\begin{pmatrix}\rho\\ \rho u\\ \rho v\\ \rho E\end{pmatrix}$, $\mathbf{F}=\begin{pmatrix}\rho u\\ \rho u^2+p\\ \rho uv\\ u(p+\rho E)\end{pmatrix}$, $\mathbf{G}=\begin{pmatrix}\rho v\\ \rho uv\\ \rho v^2+p\\ v(p+\rho E)\end{pmatrix}$, $\mathbf{V_x}=\frac{M_1}{\mathrm{Re}_{\theta 1}}\begin{pmatrix}0\\ \tau_{xx}\\ \tau_{xy}\\ u\tau_{xx}+v\tau_{xy}-q_x/\mathrm{Pr}\end{pmatrix}$, and $\mathbf{V_y}=\frac{M_1}{\mathrm{Re}_{\theta 1}}\begin{pmatrix}0\\ \tau_{xy}\\ \tau_{yy}\\ u\tau_{xy}+v\tau_{yy}-q_y/\mathrm{Pr}\end{pmatrix}$.

The lower stream has free stream Mach number $M_1=0.6$ with a boundary layer momentum thickness θ_1 while the upper stream has free stream Mach number $M_2=0.1$ with momentum thickness $\theta_2=\theta_1$ and plate width is $2\theta_1$. Initial pressure pulse and acoustic/vortical disturbance ares imposed in a steady state mean flow. Finally, initial value problems are solved for each case. The initiated pressure pulse and acoustic/vortical disturbances are defined as follows:

ⓐ *Initial value problem of a pressure pulse:*

$$\begin{pmatrix}\rho\\ \rho u\\ \rho v\\ pE\end{pmatrix}=\begin{pmatrix}\rho_0\\ \rho_0 u_0\\ \rho_0 v_0\\ \rho_0 E_0\end{pmatrix}+\begin{pmatrix}0\\ 0\\ 0\\ 0.05/\gamma\cdot\exp(-\ln(2)\cdot(((x+20)/4)^2+((y+20)/4)^2))\end{pmatrix}$$

ⓑ *Initial value problem of a initiated vortical disturbance:*

$$\begin{pmatrix}\rho\\ u\\ v\\ p\end{pmatrix}=\begin{pmatrix}\rho_0\\ u_0\\ v_0\\ p_0\end{pmatrix}+\begin{pmatrix}(1-(\gamma-1)/2\cdot M_v^{\,2}\exp(1-(\gamma/\sigma)^2))^{1/(\gamma-1)}-1\\ -M_v(y-y_0)\exp((1-(\gamma/\sigma)^2)/2)\\ M_v(x-x_0)\exp((1-(\gamma/\sigma)^2)/2)\\ ((1-(\gamma-1)/2\cdot M_v^{\,2}\exp(1-(\gamma/\sigma)^2))^{\gamma/(\gamma-1)}-1)/\gamma\end{pmatrix}$$

where $x_0=-35$, $y_0=-8$, $\gamma=1.4$ $M_v=0.1$, $\sigma=1$ *and* $r=\sqrt{(x+35)^2+(y+8)^2}$)

3. NUMERICAL METHODS

3.1. Solution Algorithm and Numerical Schemes

The wave propagation itself is hardly affected by viscosity and contribution of sound perturbations to the convection velocity of flow is negligible. Furthermore, nonlinear terms are generally small. Therefore, sound propagation is essentially described by linearized Euler equation.

$$\frac{\partial U}{\partial t}+\frac{\partial E}{\partial x}+\frac{\partial F}{\partial y}+H=S \tag{2}$$

where $\mathbf{U}=\begin{pmatrix}\rho'\\ \rho_0 u'\\ \rho_0 v'\\ p'\end{pmatrix}$, $\mathbf{E}=\begin{pmatrix}\rho' u_0+\rho_0 u'\\ u_0\rho_0 u'+p'\\ u_0\rho_0 v'\\ u_0 p'+\gamma p_0 u'\end{pmatrix}$, $\mathbf{F}=\begin{pmatrix}\rho' v_0+\rho_0 v'\\ v_0\rho_0 u'\\ v_0\rho_0 v'+p'\\ v_0 p'+\gamma p_0 v'\end{pmatrix}$, and $\mathbf{H}=\begin{pmatrix}0\\ (\rho_0 u'+\rho' u_0)\partial u_0/\partial x+(\rho_0 v'+\rho' v_0)\partial u_0/\partial y\\ (\rho_0 u'+\rho' u_0)\partial v_0/\partial x+(\rho_0 v'+\rho' v_0)\partial v_0/\partial y\\ (\gamma-1)(p'\nabla\cdot v_0-u'\partial p_0/\partial x-v'\partial p_0/\partial y)\end{pmatrix}$.

Here, **U** is the unknown vector, **E** and **F** are the linear flux vectors and the vector **H** consists of mean flow gradient terms, which are equal to zero when mean flow is uniform. The vector **S** represents possible unsteady sources in the flow. For the efficient description of later numerical results, some terms are defined such that Full Linearized Euler Equation (FLEE) represents Eq. (2) and Simplified Linearized Euler Equations (SLEE) is defined as without **H**. The SLEE is proposed by Bogey et al. (ref. 5) to suppress the instability waves in shear layer problem. In section 4, the results of FLEE will be compared with results of SLEE.

In present problem, Hybrid method (CFD for the base mean flow + CAA for acoustic scattering) is utilized. The solution procedure for trailing edge scattering problem has two parts. First, a steady mean flow solution to governing equation (1) is determined by 2D compressible laminar Navier-Stokes solution. Then acoustic simulations are carried out with the linearized Euler equation with the prescribed base flow and initial disturbances. The time dependent Euler equations (2) are discretized in space using the GODRP scheme (ref. 2) together with selective artificial damping (ref. 6) to damp out numerical oscillations and fourth order dissipation to suppress high-frequency modes. Temporal integration of the discretized equations is carried out using the third order explicit Adams-Bashford method (ref. 6). In this problem, the used grid was a H-hype rectangular grid with 601×401 in the background block and 266×45 in body-fitted block, which computational mesh is built up from a non-uniform grid clustered around the shear layer.

3.2. Boundary Condition Formulation

Because the computational domain is usually finite, boundary conditions must be imposed at the edge of the grid. These boundary conditions can generate undesirable spurious fluctuations. Therefore, accurate nonreflecting boundary conditions are necessary for computational aeroacoustics. On the surfaces, the slip boundary condition is enforced by the ghost point method. The contents in detail are introduced.

Solid Wall Boundary Conditions

Solid wall boundary (Fig. 1 ⑤) is mainly implemented by setting normal gradient of pressure at the solid wall faces equal to zero. Many methods have been developed and are useful for treating wall boundaries. Some of the more recent work in this area has been implemented by Tam & Dong (ref. 7). Tam & Dong developed wall boundary conditions with their Dispersion Relation Preserving (DRP) scheme and this method minimizes the number of required ghost values. An analysis of these conditions shows that they are capable of numerically simulating the presence of a solid wall without introducing significant errors associated with spurious numerical wave generation and numerical boundary layers. Therefore, the wall conditions implemented here are based on the approach by Tam & Dong. To set the normal pressure derivative to zero, a ghost point was used inside the wall for only the normal pressure derivative. Following equation is derived from momentum equations and setting the normal velocity at wall to zero.

$$\frac{\partial p'}{\partial n}=-\frac{1}{(\eta_x{}^2+\eta_y{}^2)}[(\eta_x\xi_x+\eta_y\xi_y)\frac{\partial p'}{\partial\xi}+\eta_x{}^2\frac{\partial}{\partial\eta}(u_0\rho_0u')+\eta_y{}^2\frac{\partial}{\partial\eta}(v_0\rho_0v') + \eta_x\eta_y(\frac{\partial}{\partial\eta}(v_0\rho_0u')+\frac{\partial}{\partial\eta}(u_0\rho_0v'))] \tag{3}$$

Inflow/Outflow Boundary Conditions & Sponge zone

The formulation of precise boundary condition is important for acoustic computation. Spurious waves generated when fluctuations leave the boundary region must be minimized. In present problem, the nonreflecting boundary condition of Tam & Dong (ref. 7) is implemented. When only acoustic fluctuation reach the boundary (for inflow and lateral boundary, Fig. 1 ①, ②, ③), the radiation boundary conditions are applied. Outflow boundary conditions (Fig. 1 ④) are also necessary when fluctuations quantities (ρ', u', v', p') reach the boundary (outflow boundary).

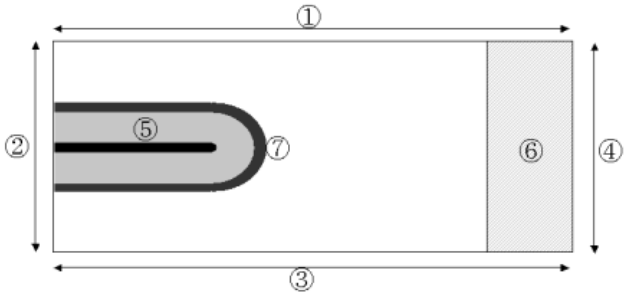

Figure. 1 Computation domain and applied boundary conditions
①,②,③: Radiation boundary condition
④ : Outflow boundary condition
⑤ : Wall boundary condition
⑥ : Sponge zone & grid stretching
⑦ : Interpolation Region

When strong vortical wave reaches the outflow boundary, this vortical wave causes an acoustic wave reflection at the outflow boundary. This spurious wave contaminates computational domain solution. For the minimization of a spurious wave, the decrease of vortical wave strength is needed at the vicinity of outflow boundary. A sponge zone (Fig. 1 ⑥) with grid stretching is then built to dissipate aerodynamic fluctuation before their reaching the outflow boundary. Larger size of sponge zone generates the smaller reflection of spurious wave. However, large size of sponge zone requires large computational domain and computational time, the selection of suitable size is important. In present problem, the sponge zone implemented by Baily & Bogey (ref. 7) is used.

4. NUMERICAL RESULTS AND DISCUSSIONS

4.1 Steady Mean Flow Results

Steady mean flow is determined by 2D Navier-Stokes Equation using Roe's scheme (ref. 8) for spatial discretization and local time stepping for time discretization to further accelerate convergence to steady state. to further accelerate convergence to steady state. Free stream conditions above the plate are $T_1=T_2$ and $\rho_1=\rho_2$. Wall boundary conditions are the no slip condition and the isothermal condition. Nonreflecting boundary condition is used at the outflow boundary.

Fig. 2 shows mean flow streamwise velocity profiles at the several lines for the mixing layer which develops downstream of the plate. Near the edge, a small wake component exists due to the co-flow stream. As the mixing layer develops downstream, the wake ingredient almost disappears and the profile becomes similar to a single inflection point shear layer. The flow profiles change rather quickly near the plate edge. Then the flow settles into a slowly growing, mildly non-parallel shear layer in further downstream.

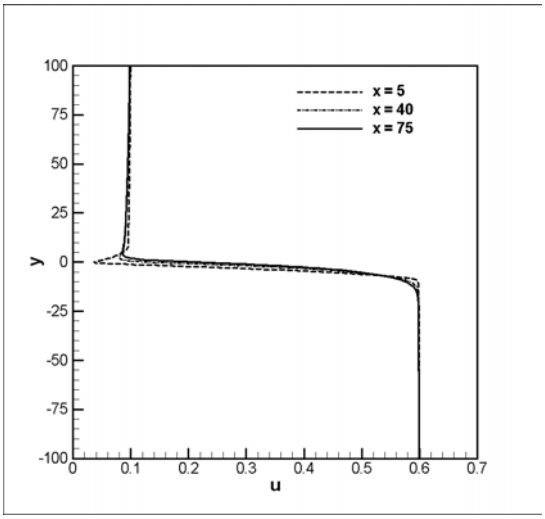

Figure. 2 Mean flow streamwise velocities profile

4.2 Acoustic Results

Overset Grids

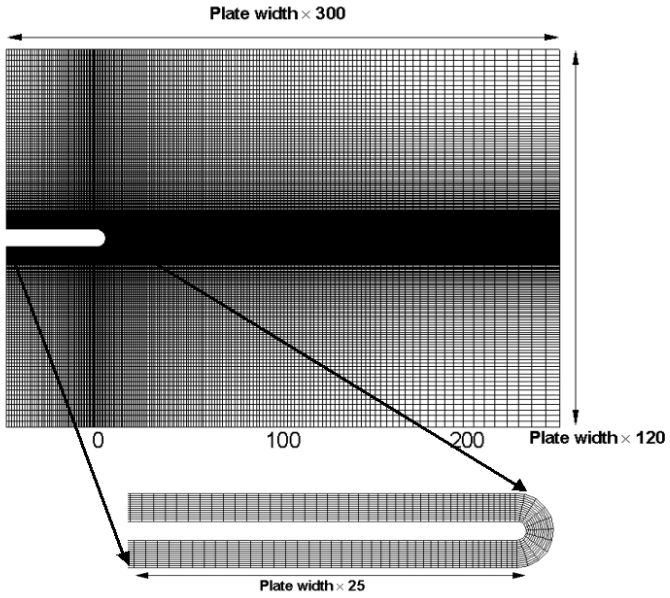

Figure. 3 Overset grids for the acoustic simulations

Construction of a single body-fitted mesh for a rounded trailing edge is very difficult. Furthermore, when the mesh is irregular or highly distorted, the numerical solutions in finite difference methods are degraded. These difficulties are overcome by the use of an overset grid technique. To retain the accuracy of the numerical schemes, high-order interpolation scheme (Fig.1 ⑦) is required for information exchange between two grid structures. In present problem, Bin's interpolation algorithm (ref. 9) is utilized.

Sound Generation by Interacting with Vortical Disturbance and Edge

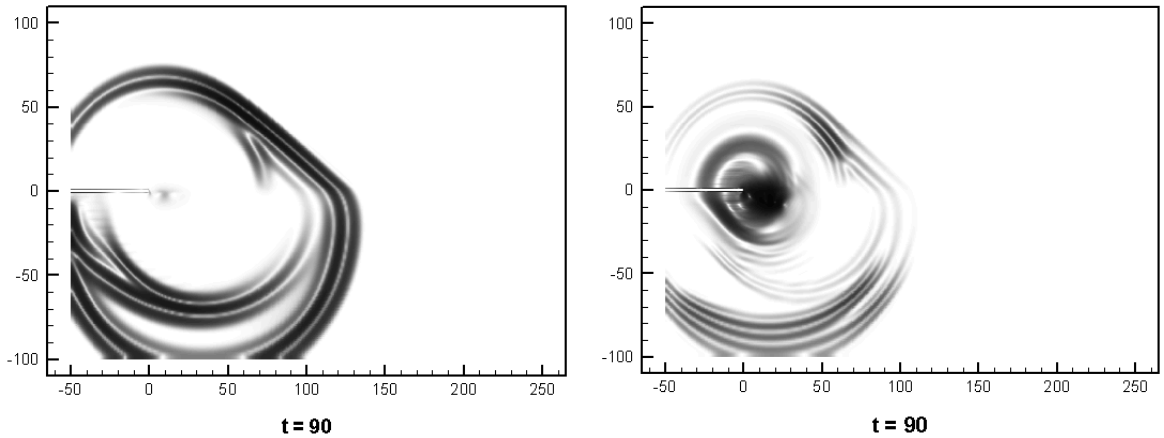

The response to pressure pulse ⓐ **The response to vortical disturbance ⓑ**

Figure. 4 Comparison of instantaneous pressure fluctuations at time = 90

Figure 4 shows the pressure distributions for the cases ⓐ and ⓑ at t = 90 by using the FLEE. When vortical disturbance is imposed on the steady mean flow, acoustic wave is generated by the interaction of the trailing edge and vorticity wave, of which phenomena cannot found in case a where only pressure pulse is imposed. However, instability waves are generated to start to flow downstream for both of cases.

Instability Waves

The amplitude of instability wave increases exponentially along streamwise (x-axis) and time. This instability waves flow to downstream with mean flow velocity, interacting with shear flow. These instability waves, which have strong strength, can cause a spurious wave reflection at the outflow boundary. So accurate outflow boundary condition and suitable size of sponge zone are required. Instability waves will go out of the computational domain at approximately t = 1400. Fig. 5 show the pressure distributions along $y = -3$ at $t = 200, 400, 600, \ldots 1200$ for initial value problem ⓑ.

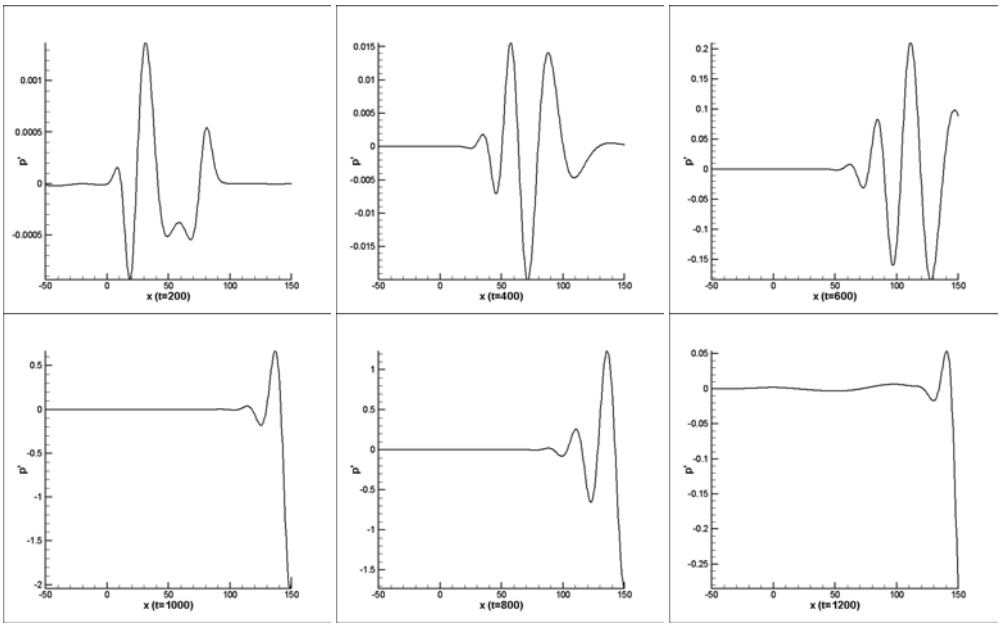

Figure. 5 Instantaneous pressure fluctuations along y = -3 at each time.

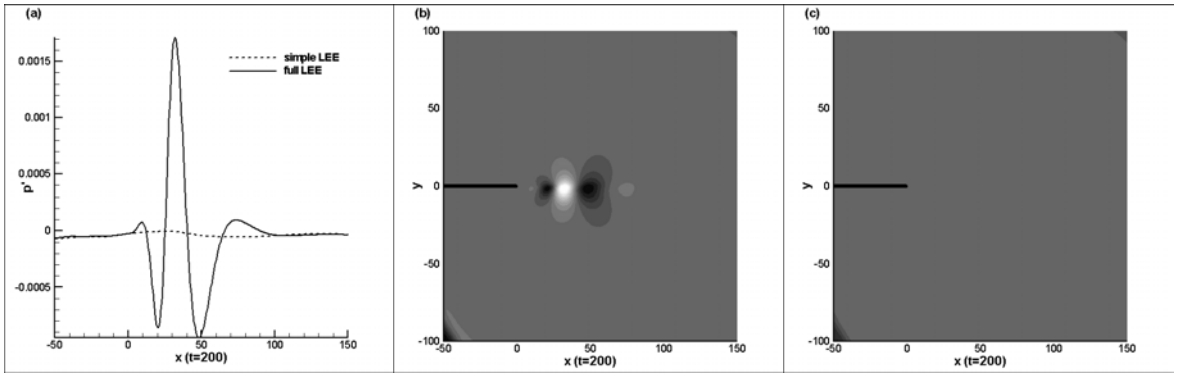

Figure. 6 Comparison of full LEE and simple LEE to pressure pulse ⓐ at t=200
(a) Instantaneous pressure fluctuation along y=-3 to full LEE and simple LEE
(b) Pressure fluctuation contour to full LEE at t=200, 15level from -0.001(black) to 0.0015(white)
(c) Pressure fluctuation contour to simple LEE at t=200, 15level from -0.001(black) to 0.0015(white)

However, it is found that the instability waves are not generated by using the SLEE for both of cases. Fig. 6 shows the comparison of the numerical results using the SLEE and the FLEE. From this figure, it is found that the

acoustic simulation using the SLEE does not generate the instability wave which exist in the results using the FLEE. The SLEE is proposed by Bogey et al. to prevent the exponential development of linear instability waves excited by source terms introduced into FLEE, through the mean shear $\partial\bar{u}_1/\partial x_2$ in the vector H. However, this instability waves are unphysical wave. But, Baron (ref. 10) shows that the same instability waves are generated by using the full Navier-Stokes equations. This means that instability wave in this benchmark problem is physical wave. From this, the mean flow gradient terms, especially the mean shear $\partial\bar{u}_1/\partial x_2$ in H, seem to play a crucial role in the instability wave generation through the interactions of the initial disturbance and the trailing edge.

Time history of the instantaneous pressure fluctuation

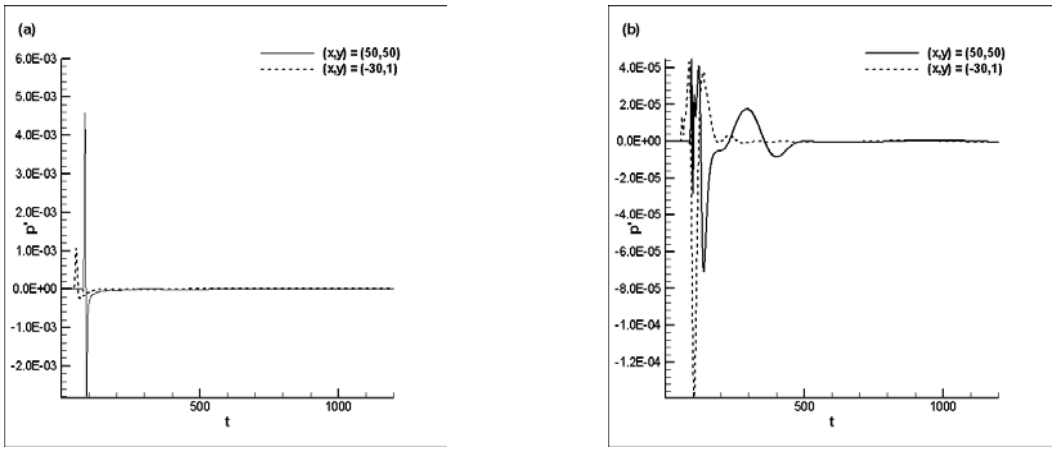

Figure. 7 Time history of the instantaneous pressure fluctuation from the FLEE
(a) The response to pressure pulse ⓐ and (b) The response to vortical disturbance ⓑ

Fig. 7 shows the time histories of pressure at the locations (-30,1) and (50, 50) for both of cases. Initial disturbance and diffracted waves are found for both of cases. However, the instabilities cannot be found in these locations. This result is also different from that of Baron et al. (please, refer to the solution comparison paper of Category 4, problem 2). It is found in our numerical simulations that the instability waves don't pass through the location (50,50) but the same thing cannot be said for that of Baron et al.. At this moment, this difference in the zone affected by the instability wave is difficult to interpret, and only one conjecture can be proposed. Baron et al. use the full Navier-Stokes equations while we use the LEE. Different terms of the governing equations, such as the nonlinear interactions and viscous terms, may affect the zone affected by the instability wave.

CONCLUSIONS

Category 4, problem 2 is solved by using the acoustic/viscous splitting techniques of which acoustic solver is governed by the LEE. CAA solver is based on the GODRP schemes to guarantee the dispersion-relation-preserving properties of the numerical scheme on the curvilinear grids. The overset grid technique is also applied to resolve complex geometries. Trailing edge scattering problem is tackled by using the FLEE and the SLEE. Through the comparison of both numerical results, it is found that the mean shear term $\partial\bar{u}_1/\partial x_2$ plays a crucial role in generating the instabilities wave in the trailing edge scattering phenomena.

Future work will be aimed at the acoustic simulation using the full Navier-Stokes Eq. and its extension to 3-dimesional engine nacelle geometries.

REFERENCES

1. Barone, M. F. and Lele, S. K.: A numerical technique for trailing edge acoustic scattering problems. *J. AIAA* , 2002-0226, 2002
2. Cheong, C. and Lee, S.: Grid-optimized dispersion-relation-preserving schemes on general geometries for computational aeroacoustics. *J. Comput. Phys.* **174**, 148 (2001)
3. Christophe Bogey.; Christophe Bailly.: Three-dimensional non-reflective boundary conditions for acoustic simulations: far field formulation and validation test cases. *ACTA ACUSTICA UNITED WITH ACUSTICA*, vol. 88, 2002
4. Tam, C.K.W.; and Dong. Z.: Radiation and Outflow Boundary Conditions for Direct Computation of Acoustic and Flow Disturbances in a Nonuniform Mean Flow. *Journal of computational Acoustics*, Vol. 4, No. 11, 1996
5. Bogey, C.; Bailly, C.; and Juve, D.: Computation of Flow Noise Using Source Terms in Linearized Euler's Equations. *J. AIAA* 40(2), 2002, pp. 235-243.
6. Tam, C.K.W.; and Webb, J.C.: Dispersion-Relation-Preserving Schemes for Computational Acoustics. *J. Comput. Phys.* **107**, 1993, pp. 262-281.
7. Tam, C.K.W.; and Dong. Z.: Wall boundary conditions for high order finite difference schemes in computational aeroacoustics. *Theor. Comput. Fluid Dyn.* **6**, 1994, pp.303-322.
8. Roe, P.L.: Approximate Riemann Solvers, Parameter Vectors and Difference Schemes. J. Comput. Phys. 43, 1981, pp. 357-372.
9. Bin, J.; Cheong, C.; and Lee, S.: Optimized Boundary Treatment for Curved Walls for High-order Computational Aeroacoustics Schemes. *J. AIAA* (In print)
10. Baron, M.F.: Receptivity of Compressible Mixing Layers, Ph. D Thesis, Stanford University, May 2003.